SENSITIVITY ANALYSIS OF RAINFALL-INDUCED SHALLOW LANDSLIDES USING TRIGRS MODEL
CASE STUDY: SAN ANTONIO DE PRADO, MEDELLÍN, COLOMBIA

LEIDY OSORIO RIOS, SILVANA MONTOYA NOGUERA, JOHNATAN RAMOS RIVERA

Artículo

Asesor, docente

Silvana Montoya Noguera

UNIVERSIDAD EAFIT

ESCUELA DE INGENIERÍAS

MAESTRÍA EN INGENIERÍA

MEDELLÍN

2021

Noname manuscript No.
(will be inserted by the editor)

Sensitivity analysis of rainfall-induced shallow landslides using TRIGRS model

Case study: San Antonio de Prado, Medellín, Colombia

Leidy Osorio-Rios · **Silvana Montoya-Noguera** · **Johnatan Ramos-Rivera**

the date of receipt and acceptance should be inserted later

Abstract Rainfall-induced landslides cause a huge number of victims each year in mountainous and tropical environments. In the last century, more than a half million families in the tropical Andean region were affected by shallow landslides, most of the time caused by heavy rainfall. An investigation about the rainfall-induced shallow landslides in San Antonio de Prado, an emerging neighborhood at the outskirts of Medellín, Antioquia, Colombia has been conducted to evaluate the effect on landslide susceptibility of changes in: (i) the geotechnical parameters, (ii) the water table position, and (iii) the different rainfall recurrence interval on stability. Transient Rainfall Infiltration and Grid-Based Regional Slope-Stability Model (TRIGRS) is used to assess the landslide susceptibility. The proposed methodology consisted of three stages: (i) model calibration, (ii) model validation, and (iii) sensitivity analysis to evaluate the effect of previous parameters and rainfall duration on stability. Stability was assessed by the fraction of failed cells of the total study area. It was found that the effect of the rain duration is significant for most cases and is more pronounced when the geotechnical parameters are reduced by one standard deviation and when the groundwater table is one meter below the sliding surface. For these cases, the fraction of failed cells increases from 3% to almost 19% after 24 hours of rainfall. In addition, the fraction of failed cells does not increase linearly with respect to the rainfall duration. The results of the validation stage suggest that the model TRIGRS can be used to assess the landslide susceptibility in Colombia, and to provide information for risk mitigation, and warning systems. However, based on the sensitivity analysis, it is necessary to conduct further research to define the geotechnical parameters for the different geological units and the water table position to deliver accurate and reliable results.

Keywords Shallow Landslides · TRIGRS · Slope stability · sensitivity analysis

Address(es) of author(s) should be given

1 Introduction

In the Colombian Andes, of 822 recorded landslides, 93.7% cause fatal consequences (Gómez et al., 2021). The Andean Mountain Range covers nearly 28% of the Colombian territory, and it is also the most densely populated region.

The city of Medellín is located at the Central Andean Range. Medellín is classified as one of the most affected regions by landslides in Colombia. In recent times, growing population and expansion of human settlements over hazardous areas have greatly increased the impact of natural disasters in the city (Aristizábal and Yokota, 2006; Aristizábal and Gómez, 2007; Klimeš and Rios Escobar, 2010; Gómez and Villarraga, 2013).

Rainfall is the most common triggering factor of landslides in Medellín, with a bimodal pattern with peaks during the rainy seasons in March - April - May and in September - October - November (Martínez et al., 2021). According to the Colombian Institute of Hydrology, Meteorology and Environmental Studies (IDEAM et al., 2015), heavy rainfalls and other extreme weather events are increasing in Colombia due to climate change, with an expected average growth of 9.3% by the end of the century, as a consequence, the probability of occurrence of landslides in the next 100 years will increase. Therefore, assessment of landslide susceptibility is an important issue.

A rational regional mapping for the susceptibility of rainfall-triggered landslides is especially necessary to provide information for hazard reduction, to aid mitigation facilities, to develop early warning systems, and to improve the management of land use (Liu and Wu, 2008).

Several applications in landslide susceptibility and hazard assessment have been published in the scientific literature to define rainfall thresholds for landslides (Alvioli et al., 2014; Vasu et al., 2016; Marin et al., 2020; Marin and Velásquez, 2020). It has been noticed that the accuracy in a landslide susceptibility and hazard assessment depends mainly on the quality and quantity of the input parameters for the physically based models, especially the geotechnical parameters - i.e. cohesion, fric-

tion angle, and soil unit weight - (Marin et al., 2021; Seefelder et al., 2017). The main objective of this study is to provide a comprehensive methodology for calibrating the input parameters for TRIGRS model (Baum et al., 2008). This methodology is later applied in a study case in San Antonio de Prado, a neighborhood at the outskirts of Medellín, Antioquia. Finally, a sensitivity analysis is performed to test the effects on the landslide susceptibility of three factors: (i) rainfall recurrence interval, (ii) geotechnical parameters, and (iii) location of the groundwater table.

2 Material and methods

2.1 TRIGRS framework model

The Transient Rainfall Infiltration and Grid-Based Regional Slope-Stability Model (TRIGRS) is a physically based model that is widely used for determining shallow precipitation-induced landslides susceptibility (Ciurleo et al., 2019; Marin et al., 2021; Xue et al., 2018). The analysis couples a hydrological model with an infinite slope stability computation to analyze the pore water pressure regime and then evaluate a distribution of factors of safety (FS) over large areas (Ciurleo et al., 2017).

2.1.1 Infiltration model

The analytical solution for unsaturated flow treats the soil as a two-layer system consisting of a saturated zone with a capillary fringe above the water table covered by an unsaturated zone that extends to the ground surface as shown in Fig.1. The unsaturated zone absorbs part of the water that infiltrates the ground surface, and the remaining water passes through this zone and accumulates above the initial water table. The unsaturated zone acts like a filter that smooths and delays the surface infiltration to other depths (Baum et al., 2008). Note that in Fig.1 the water table is above the basal boundary, i.e. $d < z_{max}$, hence the sliding mass has both a saturated and an unsaturated zone.

The Richard's equation is used to calculate the soil transient infiltration for saturated and unsaturated soil conditions. ψ is the groundwater pressure head depending on depth Z and time t. ψ is calculated as follows:

$$\frac{\partial \theta}{\partial t} = \frac{\partial}{\partial Z}\left[K(\psi)\left(\frac{1}{\cos^2\delta}\frac{\partial \psi}{\partial Z} - 1\right)\right] \tag{1}$$

where θ is the volumetric water content and $K(\psi)$ is the soil's hydraulic conductivity function, expressed in terms of the saturated hydraulic conductivity (K_{sat}) and the soil water retention curve $(SWRC)$ parameters described by the Gardner (1958) model.

$$K(\psi) = K_{sat}\exp(\alpha\psi^*) \tag{2}$$

$$\theta = \theta_r + (\theta_{sat} - \theta_r)\exp(\alpha\psi^*) \tag{3}$$

where $\psi^* = \psi - \psi_0$, ψ_0 is a constant defined below, θ_r is the residual water content, θ_{sat} is the water content at saturation, and α is a fitting parameter.

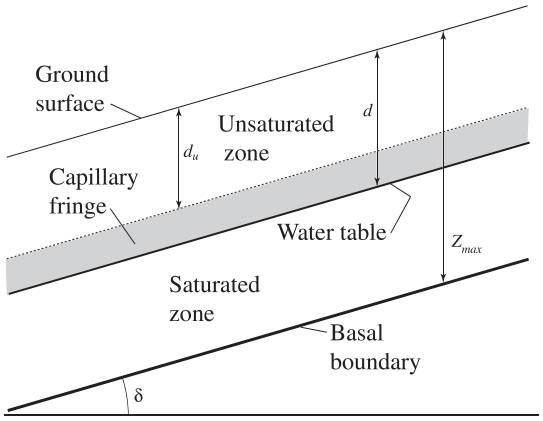

Fig. 1: Shallow groundwater table conditions in hillside soils (Baum et al., 2008)

2.1.2 Slope Stability model

Following Iverson, 2000, the slope stability model uses the infinite-slope stability method. In this method, failure of an infinite slope is characterized by the ratio of resisting basal strength to gravitational downslope basal driving shear stress (Baum et al., 2008). FS is calculated as follows:

$$FS(Z,t) = \frac{\tan\phi'}{\tan\delta} + \frac{c' - \psi(Z,t)\gamma_w\tan\phi'}{\gamma_K Z\sin\delta\cos\delta} \tag{4}$$

in which c' is the effective cohesion, ϕ' is the effective friction angle, δ is the slope angle, γ_w is the groundwater unit weight, and γ_K is the Bulk's unit weight. FS$=1$ means that the slope is in static equilibrium. Values of FS<1 indicate potential failure (in reality, such slopes do not exist), values of FS>1 indicate stable slopes.

3 Methodology

TRIGRS model is used to assess the landslide susceptibility in the study area. The proposed methodology starts with the calibration of the model and ends with a sensitivity analysis to evaluate the effect on landslide susceptibility due to changes in the geotechnical parameters, the water table position and the different rainfall recurrence interval on stability. The proposed methodology is depicted in Fig. 2 and consists of three stages: (i) model calibration, (ii) model validation, and (iii) the sensitivity analysis.

The main goals of the model calibration are (i) to identify the optimum landslide depth, and (ii) to define the mean value of geotechnical parameters in dry conditions. The main goal of the second stage is to validate that the base model found in the previous stage accurately predicts landslides during a 3 hours rainfall that were identified on the landslide inventory. In the third stage, different susceptibility maps of shallow landslides are obtained for various cases varying the three factors, previously mentioned.

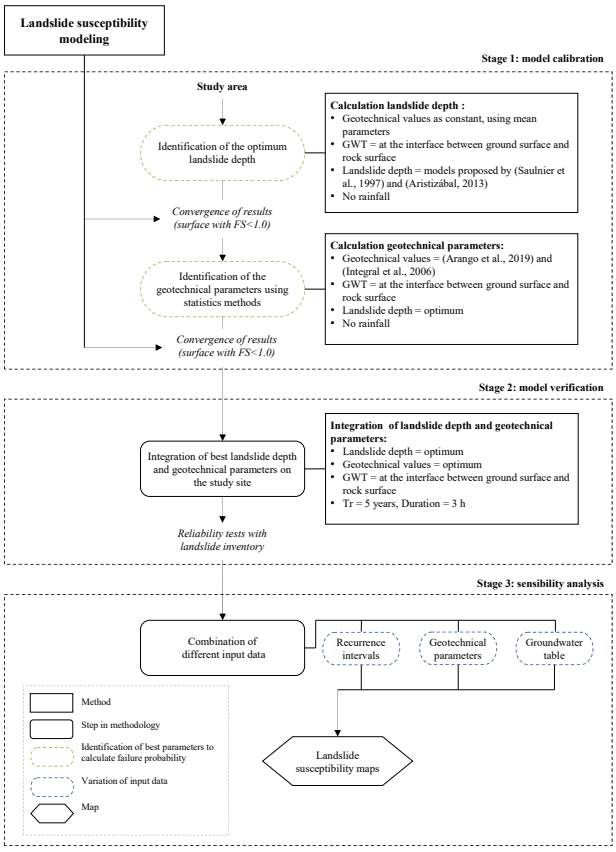

Fig. 2: Methodology for the calibration and validation of landslide susceptibility maps computed with TRIGRS

3.1 Stage 1: model calibration

The analysis starts by maintaining a given set of geotechnical parameters (c', φ, γ_s) and constant groundwater table for different soil depth, and check whether these conditions resulted in landslides, i.e. if at least 10% of the grid-cells in the study site presented $FS < 1.0$ before rainfall (Alvioli et al., 2014). In the second step, the procedure was repeated by maintaining the optimum landslide depth for different geotechnical parameters. At the end of the procedure, a set of mean geotechnical parameters and soil thickness were obtained.

3.2 Stage 2: model validation

To evaluate model calibration performance, the results obtained were compared against the inventory of observed landslides using reliability tests, based on the methods proposed by (Vandromme et al., 2020), that consists of calculating relative error (ξ), area under curve (ROC), correct classification rate (CCR), kappa index (κ) and false positive rate (FPr).

The reliability tests used to assess the different computed landslide susceptibility maps are explained in Table 1. In these tests, O_L is the observed landslide cells, i.e. the number of cells representing the landslide triggering area); P_L is the predicted landslide cells, which is the number of cells predicted in the high and very high susceptibility class $FS > 1$); N is the number of cells in the study area; a is the True positives (i.e. number of cells with $FS < 1$ and contained in observed landslide cells); b is the False positives (i.e. number of cells with $FS < 1$ and not contained in observed landslide cells) ; c is the False negatives (i.e. number of cells with $FS > 1$ and contained in observed landslide cells); and d is the True negatives (i.e. number of cells with $FS > 1$ and not contained in observed landslides cells).

Table 1: Reliability tests used to assess the different computed landslide susceptibility maps (Vandromme et al., 2020)

Test	Description	Equation
Relative error (ξ)	The uncertainty of measurement compared to the size of the measurement	$(O_L - P_L)/O_L$
ROC(AUC)	Receiver Operating Characteristic Curve (Fawcett, 2006) between the landslide occurrence probability and landslide triggering areas	–
CCR	Proportion of correctly classified observations	(a + d)/N
Kappa (κ)	Proportion of specific agreement	[(a + d) – (((a + c)(a + b) + (b + d)(c + d))/N)]/[N – (((a + c)(a + b)+(b + d)(c + d))/N]
FPr	Proportion of incorrectly classified observations	(b + c)/N

3.3 Stage 3: sensitivity analysis

The optimum soil depth and geotechnical parameters defined in stage 1 were integrated into the whole study area to calculate landslides susceptibility maps. Different scenarios of analysis were taken into consideration, varying recurrence intervals, geotechnical parameters, and groundwater table. Three variations were considered for each one of these input data, resulting in 27 cases (Table 6).

Table 2: Cases

Tr=5 years			Tr=20 years			Tr=100 years		
A1	P1	GWT1	**A10**	P1	GWT1	**A19**	P1	GWT1
A2	P1	GWT2	**A11**	P1	GWT2	**A20**	P1	GWT2
A3	P1	GWT3	**A12**	P1	GWT3	**A21**	P1	GWT3
A4	P2	GWT1	**A13**	P2	GWT1	**A22**	P2	GWT1
A5	P2	GWT2	**A14**	P2	GWT2	**A23**	P2	GWT2
A6	P2	GWT3	**A15**	P2	GWT3	**A24**	P2	GWT3
A7	P3	GWT1	**A16**	P3	GWT1	**A25**	P3	GWT1
A8	P3	GWT2	**A17**	P3	GWT2	**A26**	P3	GWT2
A9	P3	GWT3	**A18**	P3	GWT3	**A27**	P3	GWT3

For each one of these cases, the FS value was evaluated at 0, 3, 6, 12 and 24 hours of rainfall to investigate the effects of rainfall duration on landslides susceptibility.

The recurrence interval scenario was implemented for 5, 20, and 100 years, with 3 hours duration intensity from the intensity - duration – frequency (IDF) curves as the reference rainfall scenario, which corresponds to a typical landslide - triggering rainfall in Medellín (Table 3).

Table 3: rainfall recurrence interval scenarios

Scenario	Years
Tr1	5
Tr2	20
Tr3	100

The geotechnical parameters scenario was implemented considering $\pm$ 0.5 standard deviation (σ) change from mean (μ) value of c', ϕ' parameters (Table 4).

Table 4: Geotechnical parameters scenarios

Scenario	Variation
P1	$\mu - 0.5\sigma$
P2	μ
P3	$\mu + 0.5\sigma$

Mean values were defined as the optimum geotechnical values from step 1, and the standard deviation was calculated using the coefficient of variation (CoV) defined as:

$$CoV(\%) = \frac{\sigma}{\mu} \times 100 \tag{5}$$

Values of coefficient of variation were derived from the literature (Ameratunga et al., 2016). CoV values used are defined as 10% for friction angle ϕ' and 20% for cohesion c'.

Three cases were considered for the variation of the groundwater table location. First, by positioning the groundwater table at the contact between the sliding soil and the rest of the soil mass (i.e. at the depth of the rupture surface), then 1 m above, and finally 1 m below this surface, in the whole study area (Table 5).

Table 5: Groundwater table scenarios

Scenario	Level
GWT1	d_{lz} + 1.0 m
GWT2	d_{lz}
GWT3	d_{lz} - 1.0 m

4 Results and discussion

4.1 Study area

4.1.1 Regional setting

Medellín is located at the northern side of the Central Range in the Colombian Andes, approximately between latitude 6°00'N to 6°30'N and longitude 75°15'W to 75°45'W as shown in Fig.3. Weather conditions in the city are those of tropical zones, with annual average temperature of 22°C, mean relative humidity of 70%, and an annual rainfall variation from 1400 mm to 2700 mm (Aristizábal et al., 2005).

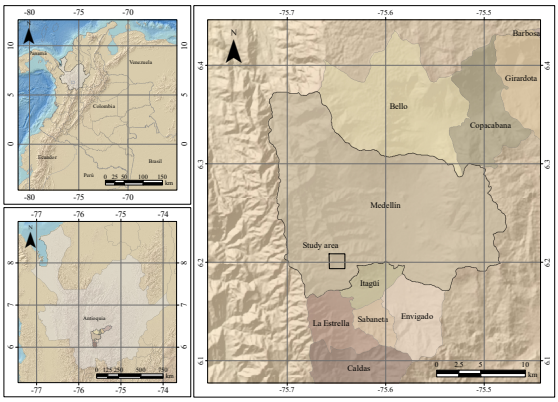

Fig. 3: Location of the city of Medellín and study site

Medellín has a varied and complex geology that has been subjected to tectonic and weathering events, with outcrops of lithological units that include rocks of different age, origin, and composition (Hidalgo Montoya and Vega Gutiérrez, 2014). Regarding age, there is a range from Paleozoic rocks to Quaternary deposits, and in terms of origin and composition as shown in Fig. 4, there are metamorphic rock such as gneiss, schist, migmatite and amphibolite; igneous rocks such as granodiorite,

dunnite, gabbro, and basalt; and volcanic-sedimentary sequence with granitic intrusions. The city is crossed by the Medellín river that spans from south to north as shown in Fig. 4. The valley slopes are mostly covered by hillslope colluvial and debris or mud flow deposits, alluvial and torrential deposits and anthropic deposits (Aristizábal et al., 2005; Integral et al., 2006).

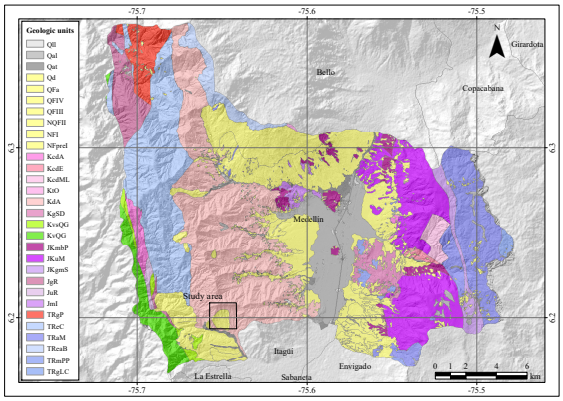

Fig. 4: Geology of Medellín
anthropic deposits (Qll), alluvial and torrential deposits (Qal, Qat), colluvial and debris or mud flow deposits (Qd, QFa, QFIV, QFIII, NFI, NFpreI), igneous rocks (KcdA, KcdE, KcdML, KtO, KdA, Kgsd), volcanic-sedimentary rocks (KvsQG, KvQG), and metamorphic rock (JKmbP, JKuM, JKgmS, JgR, JuR, JmI, TRgP, TReC, TRaM, TReaB, TRmPP, TRgLC). The study site is marked with a rectangle.

The region of interest defined for this study is located in the south side of Medellín, in the vicinity of San Antonio de Prado municipality, and covers an area of approximately 3 km^2, as shown in black rectangles in both Figs. 3 and 4. San Antonio de Prado municipality has mainly mountainous morphology, with water table conditions varying during the dry and rainy seasons, where the terrain slopes and soils constantly change due to topographic and hydraulic conditions, and the advance of physical - chemical processes of alteration of the existing soils and rocks. These changes in slopes and soils behavior generate favorable conditions to trigger landslides (Soriano et al., 2017).

4.1.2 Geological setting

The region of interest is divided into two surface geological units: debris and mud flow deposits (Qd), and Altavista Stock (KdA) (as shown in Fig. 5 shaded with yellow and pink, respectively). Debris and mud flow deposits are made up of several generations of flows, that are formed because of saturation and loss of shear strength of soils towards high slopes. Landslides on these deposits are more vulnerable to high rainfall and seismic events. Altavista Stock is a plutonic to subvolcanic igneous body that outcrops extensively on the western flank of the city. In general, these rocks are intensely weathered, with soil deposits that can reach thicknesses of 45 m at the valley, and whose texture and granulometry depend on the facies to which the parent rock corresponds (Integral et al., 2006).

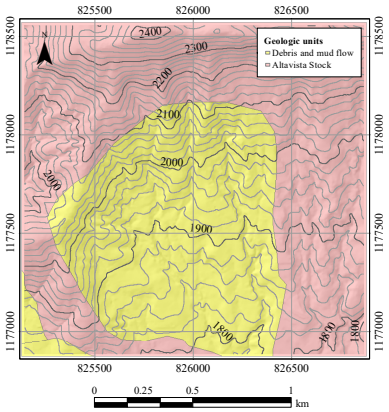

Fig. 5: Geological units in the study area

4.1.3 Landslide's inventory

The landscape evidences the occurrence of hillslope processes such as erosion and different landslide types. The available data about processes localization were obtained from the geological engineering investigation for landslides conducted by students of the Universidad Nacional de Colombia in 2019 and are shown in red in Fig. 6. Regarding the geological units shown previously, processes were identified at both units, mainly at lower altitudes.

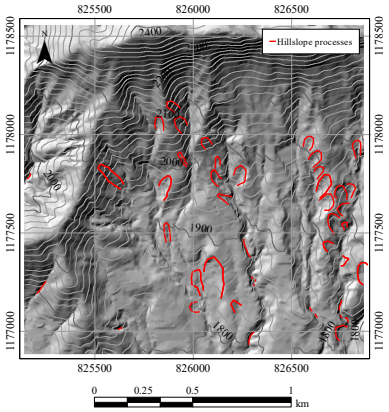

Fig. 6: Localization of the hillslope processes

4.1.4 Topographic factors

The topographic factors of elevation, slope, and flow directions, were calculated by GIS software from a 2 × 2 m digital elevation model (DEM) conducted in 2014 and are shown in Fig. 7. The elevation (Fig. 7a) varies between 1770 and 2420 m above the mean sea level. The slope (Fig. 7b) can be classified as moderate to moderately steep, with slope angles mainly between 10° and 45°, and maximum values of 60°. The flow direction (Fig. 7c) and flow accumulation (Fig. 7d) are used for the infiltration model and will be key aspects for analysis of long duration and for risk analysis.

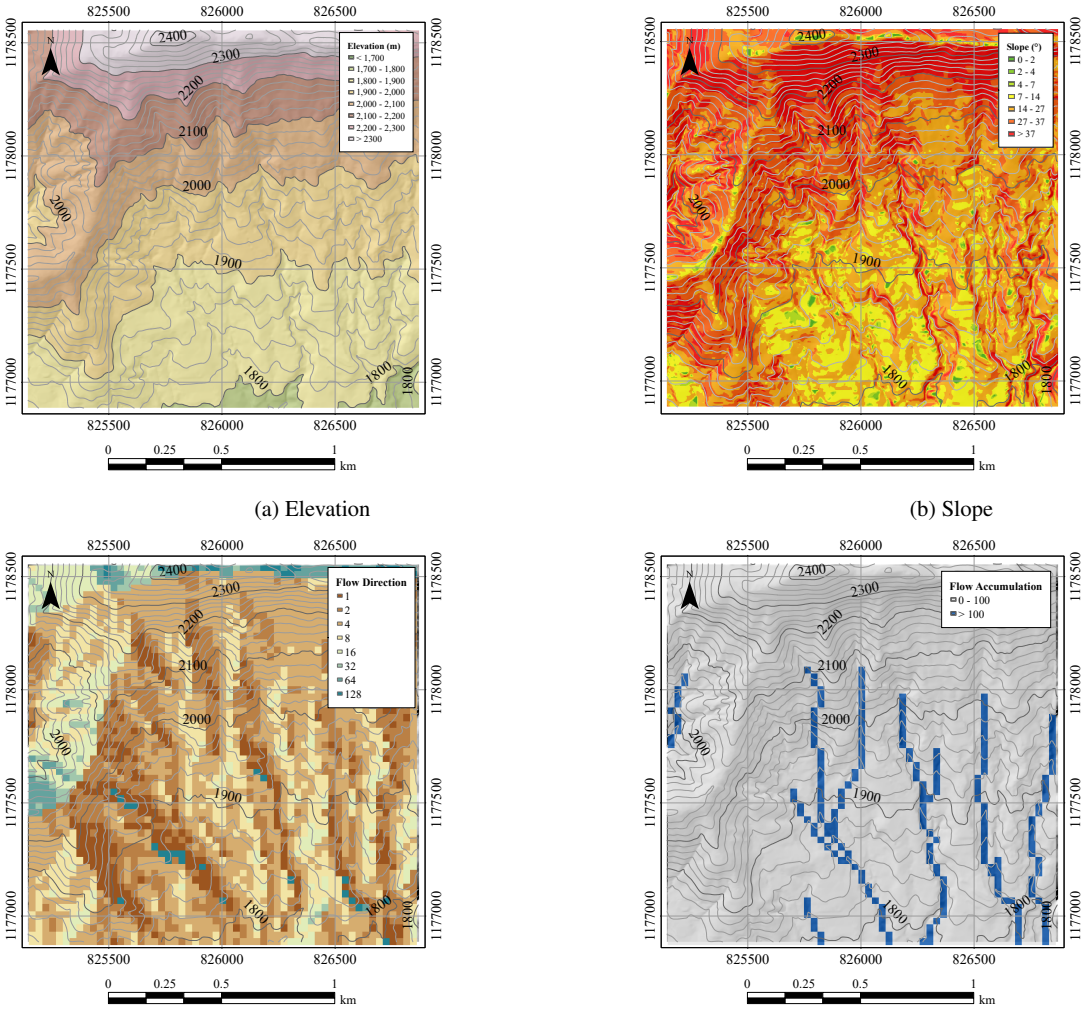

(a) Elevation

(b) Slope

(c) Flow direction

(d) Flow accumulation

Fig. 7: Topographic factors for the study site obtained with ArcGIS

4.1.5 Groundwater table

The initial groundwater table was assumed to be located at the same depth of the interface between the sliding soil and the rest of the soil mass (i.e. at the depth of the rupture surface), as used by various authors in the simulations with TRIGRS (Liu and Wu, 2008; Hidalgo Montoya and Vega Gutiérrez, 2014; Sarma et al., 2020; Marin and Velásquez, 2020; Viet et al., 2017)

4.1.6 Hydraulic parameters

The hydraulic parameters, i.e. conductivity (K_s), diffusivity (D_0), and initial infiltration rate (I_Z) are factors that affect significantly the transient fluid pressure (Liu and Wu, 2008). However, there are important uncertainties in their determination (Park et al., 2013). The values of hydraulic conductivity used in this study were taken from Ameratunga et al., 2016, and Arango et al., 2019.

If the soil is saturated, (I_Z) is equal to the hydraulic conductivity, and it reaches zero for dry soil. In this research, the value is set to $0.01K_s$, as used by various authors in the simulations with TRIGRS (Liu and Wu, 2008), (Park et al., 2013). The saturated hydraulic diffusivity (D_0) has been estimated between 2 and 500 times the K_s value. In this study, D_0 is defined as $100K_s$, as in different landslide susceptibility analysis using TRIGRS (Viet et al., 2017, Marin and Velásquez, 2020).

The soil water retention curve (SWRC) parameters for the Gardner, 1958, model, i.e. saturated volumetric water content (θ_s), residual volumetric water content (θ_r), and the inverse of the vertical height of the capillary fringe above the water table (α), were adjusted using the values of the parameters for tropical soils proposed by Hodnett and Tomasella, 2002. The soil types of the geological units were grouped according to their engineering classification (Unified Soil Classification System, USCS) in order to be consistent with the soil textural classes of the United States Department of Agriculture (USDA).

The hydraulic parameters used in this study are shown in Table 6 for both geological units. As can be seen in the table below, the Altavista Stock has higher hydraulic parameters than those for the Debris and mud flow. Among these, perhaps the most significant change is in the saturated hydraulic conductivity being more than two orders of magnitude less than the Altavista Stock, which will determine a slower change in pore-water pressure. In other words, the landslide susceptibility change with time will be less significant for Altavista Stock areas.

Table 6: Hydraulic parameters

Parameter	**Units**	**Debris and mud flow**	**Altavista Stock**
Saturated hydraulic conductivity, (K_s)	m/s	1.0E-4	4.0E-6
Hydraulic diffusivity, (D_0)	m^2/s	1.0E-2	4.0E-4
Steady infiltration rate, (I_Z)	m^2/s	1.0E-7	4.0E-9
Saturated volumetric water content, (θ_s)	m^3/m^3	0.413	0.601
Residual volumetric water content, (θ_r)	m^3/m^3	0.149	0.223

4.1.7 Rainfall data

Rainfall data is needed for determination of the ground surface flux for transient modeling of infiltration. There is one meteorological monitoring station (San Antonio de Prado) in the study area, operated by Empresas Públicas de Medellín (EPM). According to this station, the rainfall distribution is mainly characterized by an average annual rainfall of 2195 mm/year, which presents the highest levels in May and the lowest one in January (Soriano et al., 2017). In this study a 3 h duration, and 5, 20, and 100 years recurrence intervals (Tr), were selected from the intensity – duration – frequency (IDF) curves. The intensity values for all rainfall recurrence intervals are shown in Table. 7.

Table 7: Rainfall data

Tr (years)	**Intensity (mm/h)**
5	20.43
20	26.86
100	36.92

4.1.8 Soil depth

Soil depth maps was calculated as a function of the slope angle, based on the effective soil depth from Saulnier et al., 1997 and Aristizábal Giraldo, 2013 models. It represents the impermeable basal boundary (vertical depth of the lower boundary, (d_{lz}) so that a permeable superficial layer overlies a less permeable substrate.

Saulnier et al., 1997 calculates the soil depth using Eq. (6)

$$d_{lz} = z_{max}\left[1 - \frac{\tan\delta - \tan\delta_{min}}{\tan\delta_{max} - \tan\delta_{min}}\left(1 - \frac{z_{min}}{z_{max}}\right)\right] \quad (6)$$

Where z_{min} and z_{max} are the minimum and maximum values of soil depth, δ is the slope angle, and δ_{min} and δ_{max} are the minimum and maximum values of slope angle. z_{min} = 0.1 m and z_{max}= 5.0 m was assumed (Hidalgo Montoya and Vega Gutiérrez, 2014).

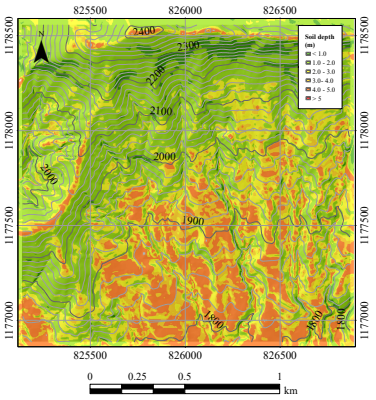

Fig. 8: Saulnier model

Aristizábal Giraldo, 2013 describes the dependence of the vertical height of the lower boundary (d_{lz}) on the slope angle (δ), as shown in Eq. (7).

$$d_{lz} = -0.026\delta + 2.83 \quad (7)$$

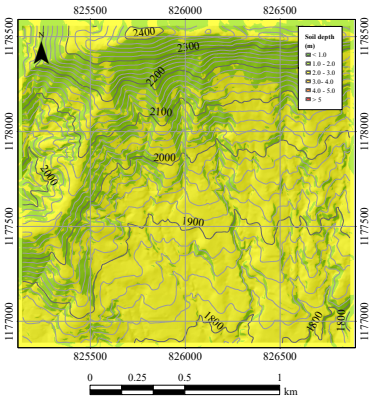

Fig. 9: Aristizábal model

Soil depth vary from 0 to 5 meters in Saulnier model and vary from 0 to 2.83 in Aristizábal model.

4.1.9 Geotechnical parameters

Geotechnical parameters were given for each material defined in the geology (c', ϕ', γ_{sat}). Table 8 summarize the geotechnical parameters evaluated in the first stage of the methodology for the two geologic units in the study area from (Integral et al., 2006) and (Arango et al., 2019), to identify the best fit which in combination with optimum soil depth model results in predicted slope instabilities.

Table 8: Geotechnical parameters

Parameter	**Units**	**P1** (Arango et al., 2019)	**P2** (Integral et al., 2006)
Altavista Stock			
Effective friction angle, (ϕ')	·	37	27
Effective cohesion, (c')	kPa	6	23
Saturated unit weight, (γ_{sat})	kN/m^3	11	17
Debris and mud flow			
Effective friction angle, (ϕ')	·	-	28
Effective cohesion, (c')	kPa	-	15
Saturated unit weight, (γ_{sat})	kN/m^3	-	19

4.2 Model calibration

The first stage of TRIGRS model application is the calibration. Soil depth models and geotechnical parameters considered for this stage are outlined below.

In accordance with the proposed methodology, once the soil depth and geotechnical parameters scenarios have been defined, the maps of susceptibility to landslide in dry conditions are calculated, first, in order to calculate optimum landslide depth and then, to calculate optimum geotechnical parameters.

In Fig. 10 initial stability conditions are shown, it is when the soil is almost dry and unsaturated, using Saulnier (Fig. 10a) and Aristizábal (Fig. 10b) model to define optimum soil depth, geotechnical parameters from Integral et al., 2006, and groundwater table at the same level as the elevation between ground surface and rock surface. At least 1% of the grid-cells (719770 total in the study area) had $FS < 1.0$ for both evaluated soil depth models, it is far less than a 10%, therefore the two models are appropriated to represent soil behavior in dry conditions.

In consequence, the optimum soil depth model was adopted, as used by various authors in the simulations with TRIGRS in Colombian areas (Marin and Velásquez, 2020, Marin et al., 2020, Marin et al., 2021). It was considered appropriate to use Saulnier model because the distribution between the maximum and minimum values of soil depth gives a greater soil thicknesses for gentle slopes and tends to significantly reduce in the steepest slopes due to the tangent of the slope angle.

To calculate optimum geotechnical parameters, Fig. 11 shows initial stability conditions when the soil is almost dry and unsaturated, using Saulnier model to calculate soil depth, geotechnical parameters from Arango et al., 2019 (Fig. 11b) and from Integral et al., 2006 (Fig. 11b), and groundwater table at the same level as the elevation between ground surface and rock surface. Failed grid-cells ($FS < 1.0$) were 0.42% and 0.35% respectively, then, the geotechnical parameters from Integral et al., 2006, with the lower percentage of failed cells were selected.

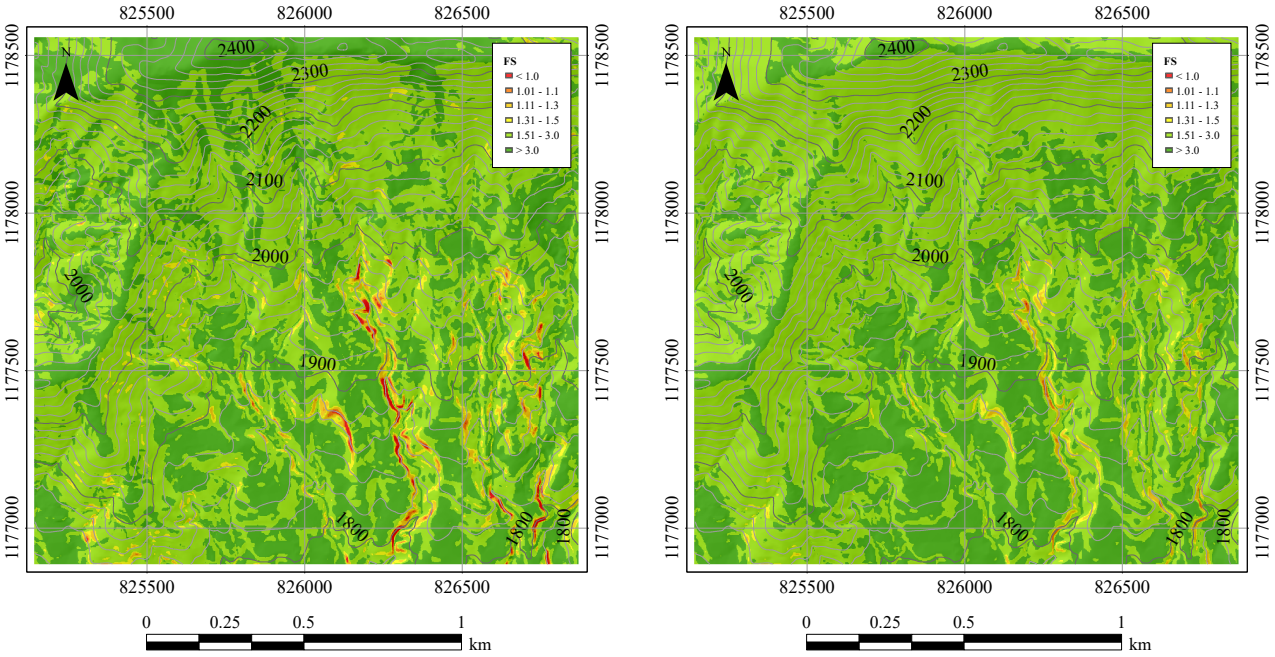

(a) Saulnier model

(b) Aristizábal model

Fig. 10: Landslides susceptibility map using different soil depth models

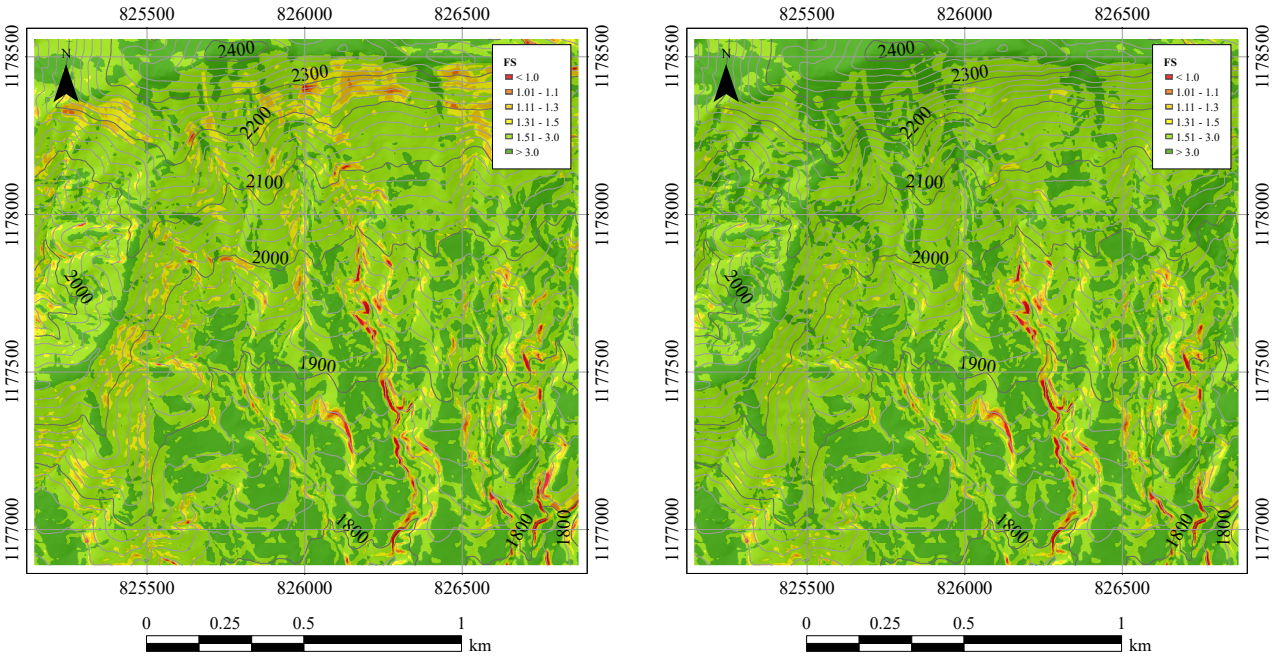

(a) P1 Arango et al., 2019

(b) P2 Integral et al., 2006

Fig. 11: Landslides susceptibility map using different geotechnical parameters

4.3 Model validation

Using the soil depth and geotechnical parameters defined in the previous calibration stage, the ability of the model to predict landslides is evaluated by means of a reliability test. This test consists in comparing landslides inventory and landslides predicted using TRIGRS model for three (3) years recurrence interval and three (3) hours of rainfall intensity. Fig. 12 shows the FS map resulting from the computation where the soil started to gain moisture and some areas are accounted as unstable. It is clear that the unstable areas obtained agree with the landslide inventory. This is considered as a good result.

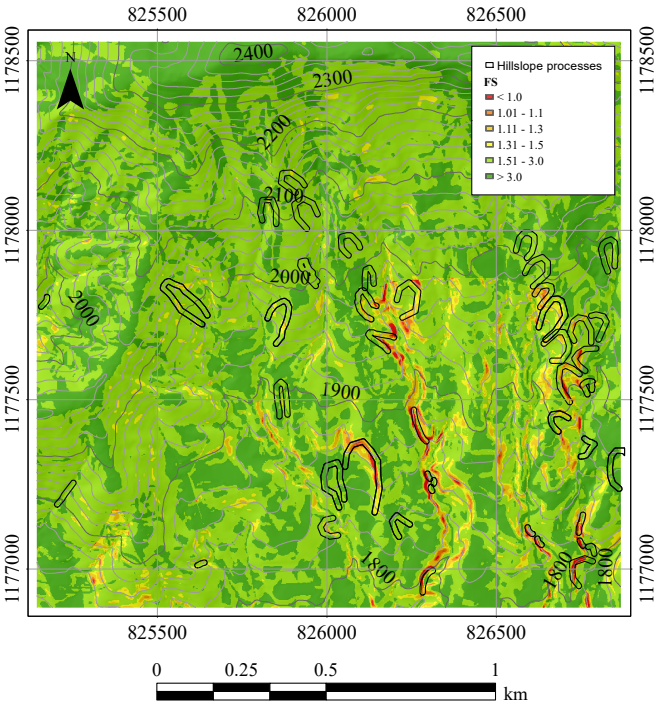

Fig. 12: Landslide susceptibility map after (3) hours of rainfall, using mean values defined in model calibration

The performance of the model is demonstrated through statistical - based reliability tests provided in Fig.13. For shallow landslides, the relative error is low (i.e. ξ = 0.28), and the correct classification rate is high (i.e. CCR = 0.96), indicating that the zones of landslide susceptibility are well recognized by the model independently of the water table location. This situation agrees with the field observations and site survey. Furthermore, the ROC (AUC) index shows high values. This is partly due to the low surface area of this type of landslide. It can be notice that all the indices stay in the ideal good fit area (i.e. the lower region in Fig. 12). Even if some errors remain, the majority of the landslides are well captured by the TRIGRS model.

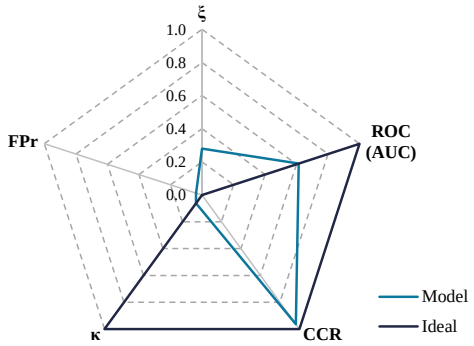

Fig. 13: Landslide reliability test

4.4 Sensitivity analysis

The sensitivity analysis consisted of evaluating the effects on the landslide susceptibility maps of three factors: (i) rainfall recurrence interval, (ii) geotechnical parameters, and (iii) groundwater table. To compare the response of the model to changes on these factors, the percentage of the cells that failed (i.e. cells with FS<1) with respect to the total cells, herein referred to as the fraction of failed cells, was evaluated for each of the 27 cases, and for 5 rainfall durations. For this study, it is clear that the effect of changing of only 1 meter on the groundwater table affects the most the number of failed cells. Thus, Fig. 14 to Fig. 16 show the results separated for groundwater table positions. In each of these figures, results of nine cases are shown, and therefore the results of all 27 cases can be analyzed. In these figures the change in markers represents the change in groundwater table (GWT), the change in line type represents the change in geotechnical parameters (P) and the change in colors represents the change in rainfall recurrence intervals (Tr).

Firstly, the effect of the rain duration is significant for almost all cases and is more pronounced when the geotechnical parameters are reduced by a-half times the standard deviation (i.e. P1), the groundwater table is one meter below the sliding surface (i.e. GWT1) and all three Tr values. For these cases, the fraction of failed cells increases from 3% to almost 19%, more than a six-fold, between no rainfall and 24 hours rainfall, as is shown in Fig. 14 with the dotted lines. In sharp contrast, when the geotechnical parameters are increased by a-half times the standard deviation (i.e. P3) and when the groundwater table is one meter above the sliding surface (i.e. GWT3), the values change from less than 0.03% to about 0.05%, over the same duration of rainfall (Fig. 16).

In addition, the fraction of failed cells does not increase linearly with respect to the rainfall duration, as shown by the change in the slope of the lines in Fig. 14 to Fig. 16, after 6 hours of rain. In other words, the behavior of the model in response to successive rainfall changes with time as the soil wetness increases. For this study, between 3 and 6 hours of rain, the fraction of failed cells varies more slowly (i.e. a more gentle slope in Fig. 14),

then, between 6 and 12 hours or 24 hours of rain, the fraction of failed slopes increases more drastically (i.e. a steeper slope) for the majority of cases analyzed. Comparing the 27 analysis cases, the change in rate varies slightly and is mostly affected by the rainfall recurrence interval as this affects the intensity rate. This change in behavior is also related to the infiltration rate, the hydraulic conductivity of the soil and the other hydraulic parameters defined in section 4.1.6. The effect of the changes on these parameters was out of the scope of this study.

Concerning the different rainfall recurrence intervals tested, the effects on the fraction of failed cells depend strongly on the groundwater table. When the groundwater table is one meter below the sliding surface (i.e. GWT3), the rainfall intensity affects more the landslide susceptibility than the change in geotechnical parameters. However, as the groundwater table is closer to the surface, the differences between cases of the same geotechnical parameters affect more the response than the rainfall recurrence interval. For example, with GWT3 (in Fig. 16) and after 24 hours of rain, for cases with the lowest geotechnical parameters (P1), a change between 5 years and 100 years in the recurrence interval presents an increase from 0.5% to almost 4%, an 8-fold increase. In addition, all values for a 100 year recurrence interval (Tr3, shown in yellow) are the greatest. In contrast, differences are less than 0.5% at 24 hours of rain, for different recurrence intervals with GWT1 as shown in Fig. 14 with different colors. In other words, the model used in this study is more strongly affected by the uncertainty on the groundwater table and on the geotechnical parameters, than on the rainfall recurrence interval.

Furthermore, as discussed previously, the change in behavior as the rainfall duration increases is slightly affected by the different recurrence intervals. For example, in Fig. 14, while at 24 hours of rain, when GWT1 is used, the results are almost the same independent on the recurrence interval, at 6 and 12 hours the lines get separated which means that the landslide susceptibility is more affected by the recurrence interval at a shorter duration than for 24 hours.

Regarding the change in the geotechnical parameters, once more its influence is affected by the groundwater table. Hence, as the groundwater table is closer to the surface, the differences in the fraction of failed cells between cases with geotechnical parameters variation, increase. For example at 12 hours with Tr2 and GWT1, the failed cells represent 3, 7 and 12 % of the total area for P1, P2 and P3, respectively (Fig. 14), but the values change to 0.5, 1.5, and 2.5 % with GWT2 (Fig. 15). Furthermore, the influence of the change in the geotechnical parameters is significant even prior to rainfall (i.e. at 0h) for GWT1, when values are 0.5, 1 and 3% for P1, P2 and P3, respectively. These results highlight the importance of accurately determining the geotechnical parameters as well as the location of the groundwater table.

Landslide susceptibility maps obtained for cases A13, A14, A14, are shown in Fig.17 for 0, 12, and 24 hours of rainfall duration. The geotechnical parameters corresponds to mean (P2), and the recurrence interval to 20 years (Tr2).

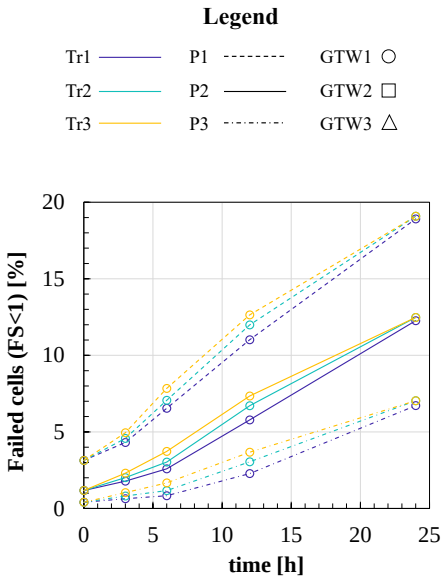

Fig. 14: Fraction of failed cells (FS<1) at increasing rainfall duration for GWT1= $d_{lz} + 1.0m$

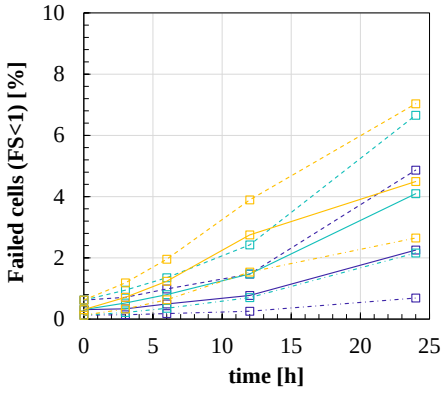

Fig. 15: Fraction of failed cells (FS<1) at increasing rainfall duration for GWT2= d_{lz}

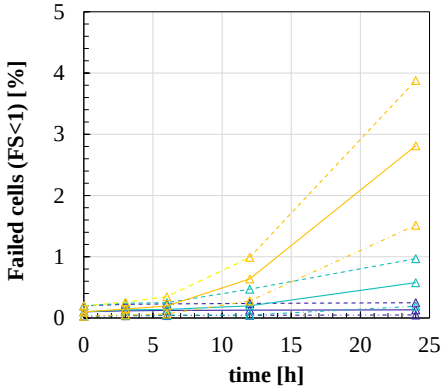

Fig. 16: Fraction of failed cells (FS<1) at increasing rainfall duration for GWT3= $d_{lz} - 1.0m$

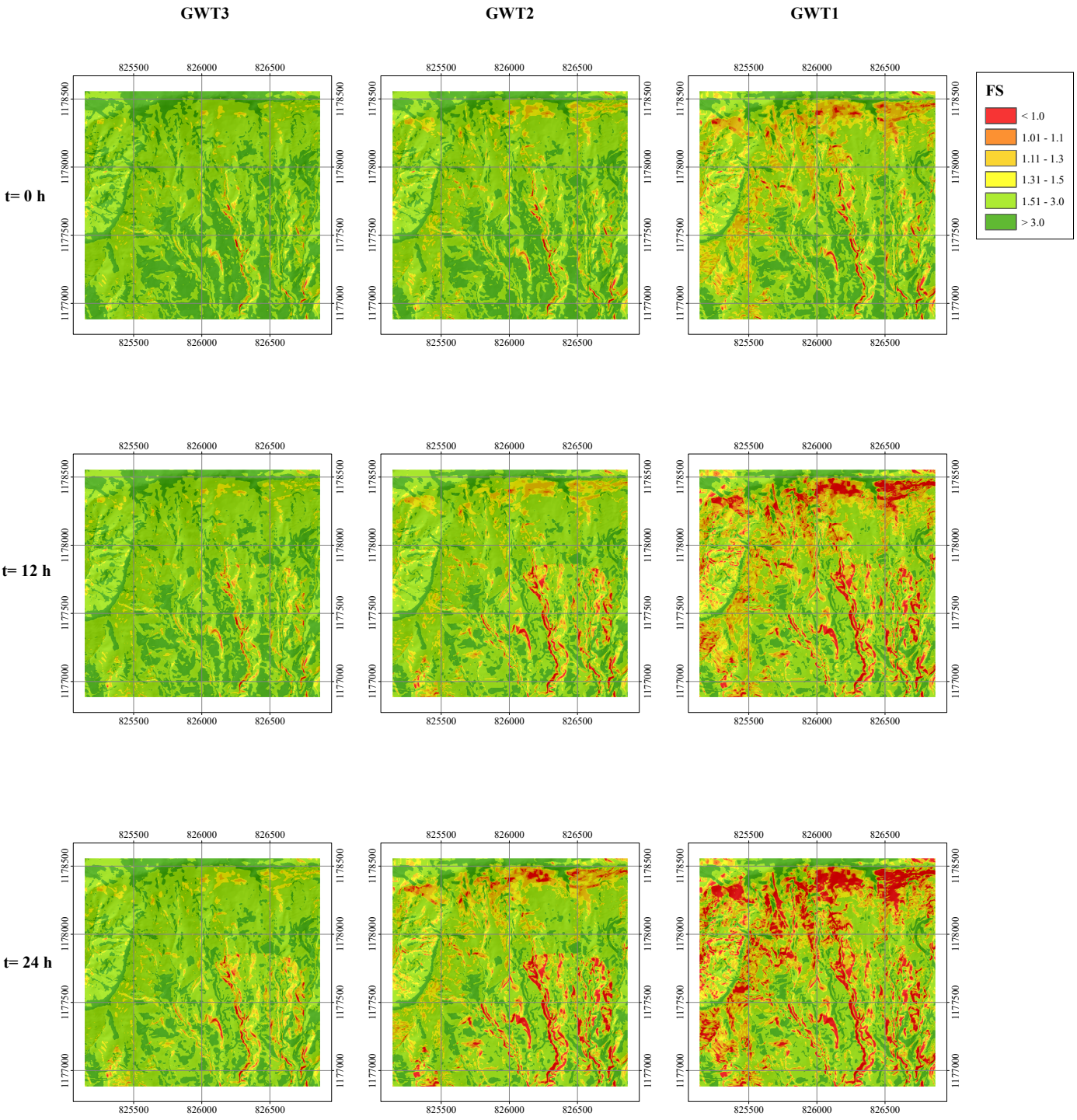

Fig. 17: Landslide susceptibility maps at increasing rainfall duration for different groundwater table positions

5 Conclusions

Rainfall-induced landslides constitute a major threat to infrastructure and casualties in steep mountainous terrain. This research consisted in evaluating the characteristics and triggering mechanisms of landslides due to rainfall in San Antonio de Prado, Antioquia, Colombia. The TRIGRS model was used to take into account the transient behavior of saturated as well as unsaturated soil conditions.

Concerning the validation of the model, the fraction of unstable cells shows a good agreement with the total area of the landslides identified in the inventory, even though they do not match exactly in terms of spatial distribution. In other words, the forecasted landslides obtained with the model seem to match in terms of several unstable cells with the real landslides, however, some pixels are wrongly located regarding the landslide scars. This spatial error would not affect risk assessment because the system would have alerted anyway for the occurrence of landslides, independently from their location. In this study, the model validation was limited as it was not possible to determine the rainfall intensity and duration that triggered the events because the landslide inventory did not include the approximate time and date of each event. More reliable and detailed landslides inventory are key to increase the accuracy of landslide models, thus fundamental for risk management in cities.

Regarding the behavior of the model in response to successive heavy rainfall, the study showed an important change with time as soon as the soil wetness increases. First, when the soil is almost dry and the rain starts infiltrating, the Factor of Safety varies gradually and more slowly.

The study revealed that the saturation of the soil at the interface between the assumed landslide depth and the underlying low permeable soil increases the positive pore water pressure, which reduces the shear strength of the soil and in turn the safety factor. Furthermore, for the particular study case, high rainfall duration contributes to accelerate the failure. In this study, hydrology plays a role in the initiation of landslides in cases where the duration exceeds 6 hours.

Concerning the effect of changes in ground water table, geotechnical parameters and rainfall recurrence intervals on the landslide susceptibility, the results highlighted the importance of accurately determining these three factors. Furthermore, these factors affect the model simultaneously thus their influence is related to the relation among them. In this study, the factor that affected the most the results was the position of the ground water table. The effect of the rainfall recurrence interval was most significant when the ground water table was 1 m below the sliding surface. But, when the ground water table was 1 m above, differences on the fraction of failed cells were mostly affected by the geotechnical parameters used. More site specific data might reduce the uncertainty in geotechnical parameters and ground water table position, thus improving the calibration and accuracy of landslide models.

The use of the methodology proposed in this study allows evaluating the performance of different approaches to improve the reliability of the landslide susceptibility models. This is an important contribution specially in lack of recognized standards and accepted practices for statistically - based landslide susceptibility modeling.

The results for this case study show the benefits of using TRIGRS model for landslide susceptibility assessment and early risk detention. Furthermore, this model could be implemented in local and regional environments as a prevention tool and as a valuable input for urban planning and early warning systems.

6 Acknowledgements

This work was financially supported by Universidad EAFIT, Vicerrectoría de Descubrimiento y Creación.

The authors would like to thank Humberto Caballero and Diego A. Rendon for providing the landslide inventory used in this research.

References

Alvioli, M., Guzzetti, F., & Rossi, M. (2014). Scaling properties of rainfall induced landslides predicted by a physically based model. *Geomorphology*, *213*, 38–47.

Ameratunga, J., Sivakugan, N., & Das, B. M. (2016). *Correlations of soil and rock properties in geotechnical engineering*. Springer.

Arango, M., Parra, M., & Hidalgo, C. (2019). Mechanical and hydraulic behaviour of unsaturated residual soils. *IOP Conference Series: Earth and Environmental Science*, *221*(1), 012016.

Aristizábal, E., & Gómez, J. (2007). Inventario de emergencias y desastres en el valle de aburrá. originados por fenómenos naturales y antrópicos en el perıodo 1880-2007. *Gestión y ambiente*, *10*(2), 17–30.

Aristizábal, E., Roser, B., & Yokota, S. (2005). Tropical chemical weathering of hillslope deposits and bedrock source in the aburrá valley, northern colombian andes. *Engineering Geology*, *81*(4), 389–406.

Aristizábal, E., & Yokota, S. (2006). Geomorfología aplicada a la ocurrencia de deslizamientos en el valle de aburra. *Dyna*, *73*.

Aristizábal Giraldo, E. V. (2013). Shia_landslide: Developing a physically based model to predict shallow landslides triggered by rainfall in tropical environments. *Escuela de Geociencias y Medio Ambiente*.

Baum, R. L., Savage, W. Z., & Godt, J. W. (2008). *Trigrs: A fortran program for transient rainfall infiltration and grid-based regional slope-stability analysis, version 2.0*. US Geological Survey Denver, CO, USA.

Ciurleo, M., Cascini, L., & Calvello, M. (2017). A comparison of statistical and deterministic methods for shallow landslide susceptibility zoning in clayey soils. *Engineering Geology*, *223*, 71–81.

Ciurleo, M., Mandaglio, M. C., & Moraci, N. (2019). Landslide susceptibility assessment by trigrs in a frequently affected shallow instability area. *Landslides*, *16*(1), 175–188.

Fawcett, T. (2006). An introduction to roc analysis. *Pattern recognition letters*, *27*(8), 861–874.

Gardner, W. (1958). Some steady-state solutions of the unsaturated moisture flow equation with application to evaporation from a water table. *Soil science*, *85*(4), 228–232.

Gómez, D., García, E., & Aristizábal, E. (2021). Spatial and temporal patterns of fatal landslides in colombia.

Gómez, E., & Villarraga, M. (2013). Recent landslides with economical and human losses in medellin city (colombia). *Landslide science and practice* (pp. 99–105). Springer.

Hidalgo Montoya, C. A., & Vega Gutiérrez, J. A. (2014). Estimation of earthquake and rainfall triggered landslides hazard (aburrá valley-colombia). *Revista EIA*, (22), 103–117.

Hodnett, M., & Tomasella, J. (2002). Marked differences between van genuchten soil water-retention parameters for temperate and tropical soils: A new water-retention pedo-transfer functions developed for tropical soils. *Geoderma*, *108*(3-4), 155–180.

IDEAM, PNUD, MADS, & DNP. (2015). *Escenarios de cambio climatico para precipitación y temperatura para Colombia 2011 - 2100 Herramientas científicas para la toma de decisiones*. IDEAM. http://documentacion.ideam.gov.co/openbiblio/bvirtual/022963/022963.htm

Integral, Universidad EAFIT, Universidad Nacional de Colombia, Inteinsa, & Solingral. (2006). *Microzonificación sísmica detallada de los municipios de Barbosa, Girardota, Copacabana, Sabaneta, La Estrella, Caldas y Envigado*. Á. https://repositorio.gestiondelriesgo.gov.co/handle/20.500.11762/19862

Iverson, R. M. (2000). Landslide triggering by rain infiltration. *Water resources research*, *36*(7), 1897–1910.

Klimeš, J., & Rios Escobar, V. (2010). A landslide susceptibility assessment in urban areas based on existing data: An example from the iguaná valley, medellın city, colombia. *Natural Hazards and Earth System Sciences*, *10*(10), 2067–2079.

Liu, C.-N., & Wu, C.-C. (2008). Mapping susceptibility of rainfall-triggered shallow landslides using a probabilistic approach. *Environmental Geology*, *55*(4), 907–915.

Marin, R. J., Garcıa, E. F., & Aristizábal, E. (2020). Effect of basin morphometric parameters on physically-based rainfall thresholds for shallow landslides. *Engineering Geology*, *278*, 105855.

Marin, R. J., & Velásquez, M. F. (2020). Influence of hydraulic properties on physically modelling slope stability and the definition of rainfall thresholds for shallow landslides. *Geomorphology*, *351*, 106976.

Marin, R. J., Velásquez, M. F., & Sánchez, O. (2021). Applicability and performance of deterministic and probabilistic physically based landslide modeling in a data-scarce environment of the colombian andes. *Journal of South American Earth Sciences*, *108*, 103175.

Martínez, H., Aristizábal, E., & García, E. (2021). A case study on causation of the landslide on 26 october 2016 in the northern colombian andes•. *Dyna (Medellin, Colombia)*, *88*, 22–30. https://doi.org/10.15446/dyna.v88n216.88600

Park, D. W., Nikhil, N., & Lee, S. (2013). Landslide and debris flow susceptibility zonation using trigrs for the 2011 seoul landslide event. *Natural Hazards and Earth System Sciences*, *13*(11), 2833–2849.

Sarma, C. P., Dey, A., & Krishna, A. M. (2020). Influence of digital elevation models on the simulation of rainfall-induced landslides in the hillslopes of guwahati, india. *Engineering Geology*, *268*, 105523.

Saulnier, G.-M., Beven, K., & Obled, C. (1997). Including spatially variable effective soil depths in topmodel. *Journal of hydrology*, *202*(1-4), 158–172.

Seefelder, C. d. L. N., Koide, S., & Mergili, M. (2017). Does parameterization influence the performance of slope stability model results? a case study in rio de janeiro, brazil. *Landslides*, *14*(4), 1389–1401.

Soriano, C., Lopera, J., & Ruiz Perez, J. (2017). Projeto de estabilização de encostas: Caso de estudo san antónio de prado – colômbia.

Vandromme, R., Thiery, Y., Bernardie, S., & Sedan, O. (2020). Alice (assessment of landslides induced by climatic events): A single tool to integrate shallow and deep landslides for susceptibility and hazard assessment. *Geomorphology*, *367*, 107307.

Vasu, N. N., Lee, S.-R., Pradhan, A. M. S., Kim, Y.-T., Kang, S.-H., & Lee, D.-H. (2016). A new approach to temporal modelling for landslide hazard assessment using an extreme rainfall induced-landslide index. *Engineering Geology*, *215*, 36–49.

Viet, T. T., Lee, G., Thu, T. M., & An, H. U. (2017). Effect of digital elevation model resolution on shallow landslide modeling using trigrs. *Natural Hazards Review*, *18*(2), 04016011.

Xue, C., Nie, G., Li, H., & Wang, J. (2018). Data assimilation with an improved particle filter and its application in the trigrs landslide model. *Natural Hazards and Earth System Sciences*, *18*(10), 2801–2807.